EXPERIMENTAL STUDY FOR THE SIZE EFFECT ON THE FLEXURAL BEHAVIOUR OF SPLWA REINFORCED CONCRETE SLABS STRENGTHENED WITH CFRP STRIPS

Ahid ZUHAIR Hamoodi
University of Basrah

EXPERIMENTAL STUDY FOR THE SIZE EFFECT ON THE FLEXURAL BEHAVIOUR OF SPLWA REINFORCED CONCRETE SLABS STRENGTHENED WITH CFRP STRIPS

By; Prof. Dr. Riadh A. Abass[1] and Mr. Ahid Z. Hamoodi[2]

[1]Dept. of civil engineering, College of engineering, University of Mothana.

[2]Dept. of civil engineering, College of engineering, University of Basrah.

ARTICLE INFO

Received:

Accepted:

Keywords

CFRP, Sand-PLWAC OWS, Monotonic Loading.

Abstract: An experimental Study was conducted to investigate the size effect on the flexural behaviour of sand-porcelinite lightweight aggregate reinforced concrete one way slabs (SPLWAC OWS). In order to get a clear results, eight slabs were casted, and six of them were strengthened with carbon fibre reinforced polymer (CFRP) strips. To investigate the size effect, four slabs were of 300 mm width, 1500 mm length and 80 mm depth and the others were of 300mm width, 2000 mm length and 108 mm depth. The present study showed that the SPLWAC OWS showed a reverse size effect. The failure mode was by yield of steel for the control un-strengthened slabs, while it was by yield of steel followed by rupture of CFRP strips for the strengthened slabs. Also, the results of this study were compared with those obtained by the ACI equations. This comparison showed that the ultimate moment strength and deflection obtained by the ACI equations were always less than those obtained experimentally.

دراسة عملية لتأثير الحجم على تصرف الانحناء للبلاطات الخرسانية المسلحة الخفيفة والمقواة بشرائح البوليمر المسلحة بألياف الكربون

الملخص: يقدم هذا البحث دراسة عملية لتأثير الحجم على سلوك الانحناء للبلاطات الخرسانية المسلحة الخفيفة. لغرض انجاز البحث، تم تحضير ثمان بلاطات، ستة منها مقواة بشرائح البوليمر المسلحة بألياف الكربون. لدراسة تأثير الحجم تم تحضير اربع بلاطات بأبعاد 300 ملم عرض، 1500ملم طول و 80 ملم سمك وأربع بلاطات بأبعاد 300 ملم عرض، 200 ملم طول و 108 ملم سمك . أظهرت هذه الدراسة تأثير عكسي للحجم على تصرف الانحناء للبلاطات. كانت طبيعة الفشل بواسطة خضوع حديد التسليح في البلاطات غير المقواة، بينما كانت طبيعة الفشل بواسطة خضوع حديد التسليح يتبعه تمزق شرائح البوليمر في البلاطات المقواة. تم مقارنة نتائج هذه الدراسة مع معادلات الكود الأمريكي وأظهرت المقارنة أن تحمل العزم الأقصى والهطول المحسوب باستخدام معادلات الكود الأمريكي كانت دائما اقل من نتائج الدراسة العملية.

الكلمات المفتاحية

ألياف الكاربون، بلاطات بأتجاه واحد خرسانية خفيفة، حمل ستاتيكي.

E-mail addresses:
mm812000@yahoo.com

Introduction

The use of fiber-reinforced polymer (FRP) composites for the rehabilitation of beams and slabs started about 30 years ago. Where FRP composites are used as external reinforcement in the rehabilitation of R.C. elements, they increase the strength and the stiffness of the structure[1]. One of the major problems in the design and execution of buildings is the considerable weight of dead load. Using lightweight materials is an effective solution to reduce dead loads and therefore reduce the dimensions of the supporting structure, minimize the earthquake force on the building and finally to increase the speed, facilitate the execution and economize the project [2]. Structural lightweight aggregate concrete (SLWAC) has an in place unit weight of 1440 to 1840 kg/m^3 compared to normal weight concrete with a density of 2240 to 2400 kg/m^3. For structural applications the cylinder compressive strength should be greater than 17.0 MPa. In most cases, the marginally higher cost of the SLWAC is offset by size reduction of structural elements, less reinforcing steel and reduction in concrete volume, resulting in lower overall cost [3]. According to ACI 318-2011, sand- lightweight aggregate concrete is the concrete in which the sand is the fine aggregate while the lightweight material represents the coarse aggregate [4]. The mechanical properties of LWAC differ significantly from those of normal weight concrete, mainly attributed to high porosity of LWA, which causes high water absorption rate and smaller modulus of elasticity of concrete. LWAC turns out weaker strength and more brittle, therefore, the study of the size effect in LWAC may help to understand the behaviour of LWAC and predict load-carrying capacity [5].

Porcelinite Lightweight Coarse Aggregate (PLWA)

Local naturally occurring lightweight aggregate (LWA) of porcelinite stone was used in this study as coarse aggregate. It was received in large lumps through the State Company of Geological Survey and Mining (SCGSM), which provide it from Al-Anbar Governorate, Akashat district, Westren Desert - Traifawi. The lumps were manually crushed into smaller sizes, screened and graded on a standard sieves series of 12.5, 9.5, and 4.75mm, complying with ASTM C330-2004 [6] as shown in Table 1 and figures 1 and 2. Since a high proportion of dust leads to segregation and causes crazing of exposed concrete [7], and due to the rapid water absorption of the LWA, the saturated surface dry (SSD) condition has been achieved by washing and spreading the aggregate in the laboratory air for a suitable time. Table (2) lists the physical and chemical properties and their corresponding proper specifications.

Figure (1): The series of the used seives.

Figure (2): The graded porcelinite aggregate.

Table (1): Selected grading of PLWA.

Sieve size (mm)	% Passing ASTM C330-2004[6]	Selected passing %
12.5	100	100
9.5	80-100	85
4.74	5-40	8
2.36	0-20	0
1.18	0-10	0

Table (2): Chemical and physical properties of PLWA [7, 8].

Property	Specification	Result
Specific gravity	ASTM C127-88	1.44
Absorption, %	ASTM C127-88	35
Dry loose unit weight, kg/m^3	ASTM C29-89	772
Dry ridded unit weight, kg/m^3	ASTM C29-89	830
Aggregate crushing value, %	BS 812 part 110-1990	16
Sulfate content (so_3), %	BS 3797 -part 2-1981	0.34
Staining materials:	ASTM C 641-82	No stain

Details of The Experimental Program

The experimental program consisted of eight one-way slabs, four of them of length 1500 mm, 300 mm width and 80 mm depth and the rest of length 2000 mm, 300 mm width and 108 mm depth. A bottom concrete cover of 20 mm was used for all slabs. The slab specimens were casted using sand-PLWAC of grade 20 MPa. After casting, the specimens were allowed to cure for about 28 days which helps the concrete to stabilize its own properties like compressive strength and modulus of elasticity. Table 3 presents the mix proportions and properties of ingredients of concrete. Tables 4,5, and 6 present the mechanical properties of steel reinforcement, physical properties of the used cement and physical properties of the used sand respectively, where all tests were carried out in the material Lab. Civil engineering department, college of engineering, Basrah university.

Table (3): The mix proportions and ingredients of the selected sand-PLWAC mix.

Mix proportion (by weight)	1:1.031:0.978
W/C (by weight)	0.41
Cement (kg/m$^{3)}$	518
Sand (kg/m^3)	534
PLWAC (kg/m$^{3)}$	506
Water (kg/m$^{3)}$	212
f_{cu} 28-day (MPa)	24.4
f_c' 28-day (MPa)	20

Table (4): Properties of steel reinforcement.

Steel Reinforcement	Test Results	ASTM A615/A615M-04b, Standard[13]
Diameter, mm	8.0	-
Yield Tensile Strength, MPa	450	Not less than 420
Ultimate Tensile Strength, MPa	675	Not less than 620
Modulus of Elasticity, MPa	200000 (**Assumed value**)	-
Elongation, %	16	Not less than 9

Table (5): Physical properties of the cement.

Physical Properties	Test Result	Limits of IOS 5:1984[14]
Fineness (m^2/kg)	312	$\geq$ 230
Setting Time Initial (hrs:min) Final (hrs:min)	 2:10 4:00	 $\geq$ 45 min $\leq$ 10 hrs
Compressive Strength 3 days (MPa) 7 days (MPa)	 20.5 28.8	 $\geq$ 15 $\geq$ 23

Table (6): Physical properties of fine aggregate.

Physical Properties	Test Result	Limits of IOS No. 45/1984 [15]
Specific Gravity	2.65	-
Sulphate Content (SO_3) %	0.33	$\leq$ 0.5
Absorption %	1.1	-
Loose bulk density kg/m^3	1645	-

CFRP Installation

The mechanical properties of CFRP and epoxy resin were presented in Tables 7 and 8. The Installation of CFRP strips was conducted under the Manufacturer Specifications [16, 17]. The concrete surface of the slabs tension face was cleaned from lousy materials by a surface cleaning machine as shown in figure 3. Firstly, the two-parts of epoxy (A and B) was mixed in 4:1 ratio and the resulting material was gray paste. The epoxy mixer has been applied to the surface of concrete at location of CFRP strips to fill the cavities and to applied the CFRP strips at the surface of concrete.

Table (7): Properties of CFRP strips [16].

Material Type: Sika Warp Hex – 230C				
Tensile Strength MPa	Elongation at failure %	Tensile Modulus GPa	Thicknes s mm	Weight (g/m2)
3500	1.5	230	0.13	225

Table (8): Properties of epoxy resin (Sikadur-330) [16].

Appearance	Density (kg/l) mixed	Pot live (minute)	Tensile strength (MPa)	Flexural modulus (MPa)
Com A: white Com B: Gray	1.31	15C:90min 35C:30min	30	3800
Mixing Ratio by Weight, A:B = 4:1				

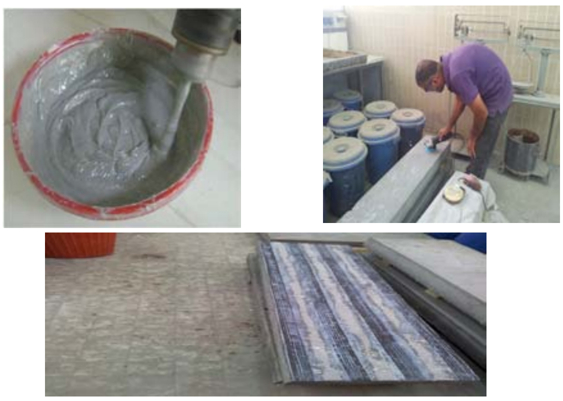

Fig. (3): Preparing and application of CFRP strips.

Experimental Set up

Eight simply supported one way slabs were tested monotonically under two line loads as shown in figures 4 and 5. All slabs were tested using a hydraulic universal testing machine with a capacity of 2000 kN. A dial gauge was used at midspan to monitor the deflection. The load was applied at a rate of 1 kN per step.

Details of Slabs

As shown in figure 6 below, the slabs details can be described as: **1. S1** and **S2**: 1.5m and 2m Control un-strengthened Sand-PLWAC OWS respectively; **2. S1CF4**: 1.5 m Sand-PLWAC OWS strengthened with one layer of four CFRP strips of 30 mm width; **3. S1CF5**: 1.5 m Sand-PLWAC OWS strengthened with one layer of five CFRP strips of 30 mm width; **4. S1CF**: 1.5 m Sand-PLWAC OWS strengthened with one layer of CFRP strip of 300 mm width; **5. S2CF6**: 2 m Sand-PLWAC OWS strengthened with one layer of six CFRP strips of 30 mm width; **7. S2CF7**: 2 m Sand-PLWAC OWS strengthened with one layer of seven CFRP strips of 30 mm, and **8. S2CF**: 2 m Sand-PLWAC OWS strengthened with one layer of CFRP strips of 300 mm width.

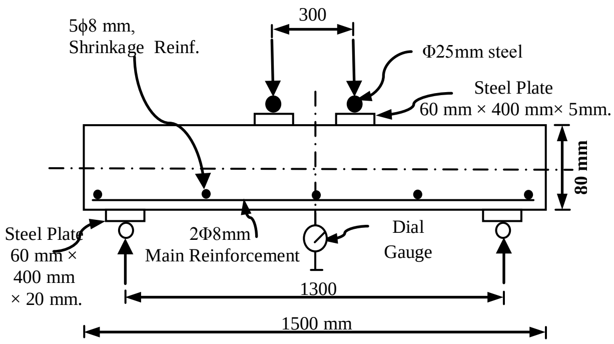

(a) 1.5 m
Fig. (4): Dimensions, Loading, Reinforcement Scheme

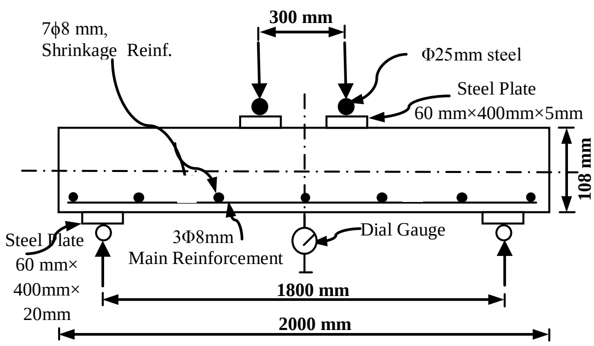

(b) 2.0 m
Fig. (4): Dimensions, Loading, Reinforcement Scheme

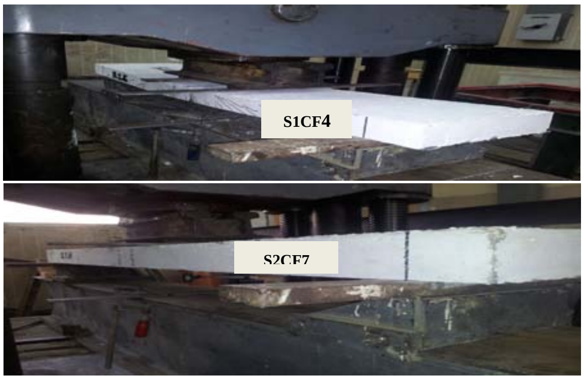

Fig. (5): Picture of the slab in the testing machine.

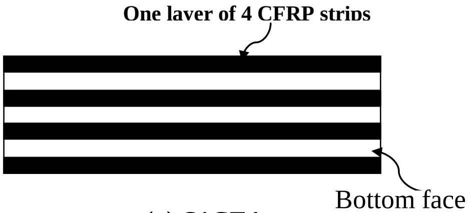

(a) S1CF4.

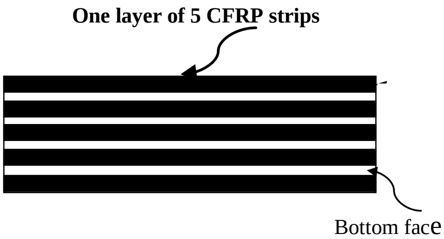

(b) S1CF5.

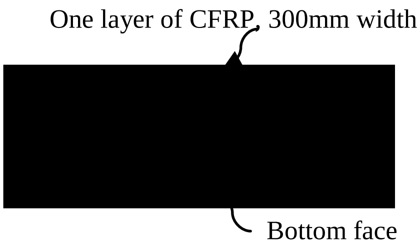

(c) S1CF and S2CF.

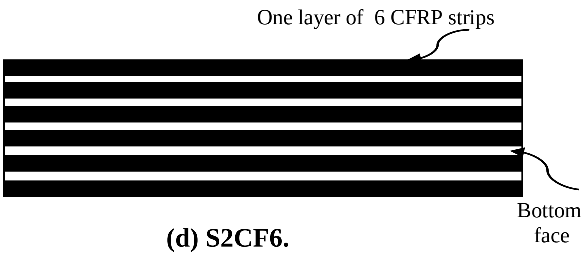

(d) S2CF6.

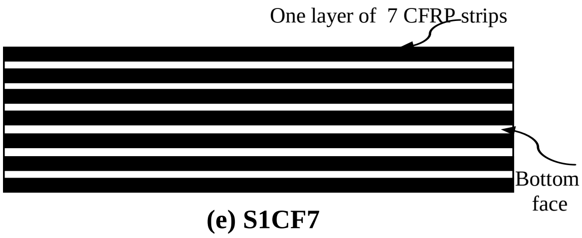

(e) S1CF7

Fig.(6): CFRP Details.

Test Results

1. General Behavior

The first visible cracking loads, ultimate loads and failure modes are presented in Table 9. The first visible flexural cracks noticed at (30.2% to 36.5%) and (31.5 to 33.3%) of failure load for the one way slab with span of 1.5 m and 2 m (OWS) respectively. These cracks appeared at the bottom surfaces whenever the tensile stresses exceed the modulus of rupture of concrete. For control un-strengthened slabs, the first crack appeared at the middle of the slab and developed across the width of the slab (i.e. parallel to the support). Further development of flexural cracks occurred parallel to this crack and propagated throughout the thickness of the slab on increasing the applied load. The flexural cracks were vertical smooth cracks initiated and propagated through the lightweight aggregates (LWA) and not around it. This is attributed to the smaller toughness of LWA, where the interfacial transition zone (ITZ) has higher tensile strength than LWA. In strengthened slabs and with increasing the applied load, the cracking phenomenon at the soffit of the slab is degenerated in a multicracking pattern with much more closely-spaced cracks. This phenomenon increased with increasing the amount of CFRP strips, with the formation of secondary cracks (small diagonal branching cracks around the flexural cracks) as a result to the relative sliding between the CFRP strips and the adjacent concrete. This behaviour is very coincident with the results obtained by Bonaldo et al.[10]. In some strengthened slabs and outside the region between the applied loads, flexural – shear cracks were formed and extended towards the applied loads. Crack pattern and failure modes for the OWS are shown in Fig. 7. For Control slabs (S1 and S2), when the load reached a value that caused yielding of steel, the deflection was increased and cracks were propagated quickly, then the load was slightly increased so that the crushing of compression face of concrete under loads occurred. These slabs failed by yielding of steel in a ductile failure mode. CFRP strengthened slabs failed by yielding of steel followed by abrupt rupture of CFRP strips. This is because that, at failure, the tensile strains developed in the CFRP strips attained its ultimate strain capacity, justifying the type of failure mode occurred in these slabs. In some cases, the rupture of CFRP strengthened slabs accompanied by delamination of concrete cover within the region between the two applied loads. This may be attributed to the lower bond characteristics of the LWAC and the bond stress (interfacial shear stress at the concrete cover-internal reinforcement interface) that was too high to develop a shear / tension failure of the concrete attached to the CFRP strip at the edge. It is observed that all strengthened OWS showed a brittle failure mode in comparison to the control un-strengthened slabs. Under static loads, the 1.5m strengthened slabs showed about (38 to 86.2%) and (66.7 to 92.5%) higher visible cracking and ultimate loads respectively than comparable control un-strengthened slab. Similarly, the 2 m strengthened slabs showed about (58.1 to 87.1%) and (31.5 to 33.0%) higher visible cracking and ultimate loads respectively than comparable control un-strengthened slab. This may be attributed to the presence of CFRP strips that share tensile strains with the concrete and hence delay the stress that exceeding the modulus of rupture of concrete (i.e. the CFRP strips restrained the tensile stresses) which lead to enhance the flexural capacity of the slab.

Table (9): Static first visible cracking and ultimate loads for sand-PLWAC OWS

Slab designa-tion	P_{cr} (kN)	P_u (kN)	$(P_u-P_{uo})/P_{uo}$ %	P_{cr}/P_u %	Failure Mode
S1	5.8	15.9	-----	36.5	YS
S1CF4	8.0	26.5	66.7	30.2	ROC
S1CF5	9.5	28.1	76.7	33.8	ROC
S1CF	10.8	30.6	92.5	35.3	ROC
S2	6.2	18.6	-----	33.3	YS
S2CF6	9.8	31.1	67.2	31.5	ROC
S2CF7	10.8	32.6	75.3	33.1	ROC
S2CF	11.6	35.1	88.7	33.0	ROC

Where:

P_{cr} : Visible Cracking Load**; P_u:** Ultimate Load**;**

YS: Yield of Steel**; ROC:** Rupture of CFRP**.**

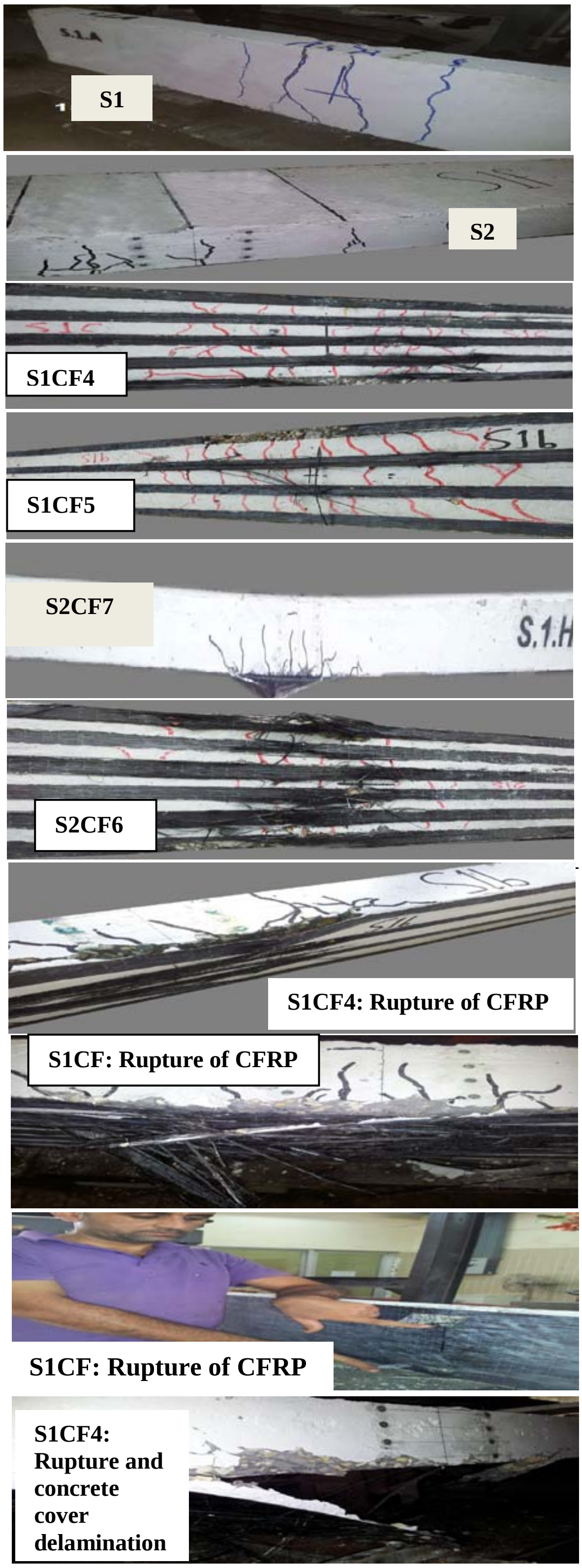

Fig. (7): Crack Patterns and Failure modes of strengthened sand-PLWAC OWS under static loading.

2. Size Effect

Two different sizes of sand-PLWAC slabs with different CFRP strips ratios were studied in this work to investigate the effect of CFRP on the flexural behaviour of slabs. The size effect of slabs was conducted by changing the length and thickness of the slab and fixing the (a/d) and steel ratios, where details of the slabs are presented in figure 4. The size effect is studied by introducing the ratio of the experimental to calculated ultimate moment of slabs with two different effective depths. The ultimate moment of the tested slabs are listed in Table 8. Also, the theoretical ultimate moment strength of the slabs, which were calculated according to **ACI 318M-11Code** [4] and **ACI 440.2R-02 report** [15], are shown in Table 10.

In the ACI code and report, the calculations are based on the equation:

For control specimens[4];

$M_n = A_s\, fy\, d\, \{1 - 0.59\, (f_y/f'_c)\, \rho\}$ …….. (1)

For strengthened specimens[15];

$M_n = A_s\, f_y\{d - (\beta_1 c / 2)\} + \psi\, A_f\, f_{fe}\, \{h - (\beta_1 c / 2)\}$ …(2)

Where:

A_S = Cross sectional area of the reinforcing steel;

f_y = Yield strength of the reinforcing steel;

f'_c = Concrete compressive strength at 28 days;

d = Effective depth of the slab; h= Thickness of the slab; ρ = Steel ratio; $\beta_1 = 1.09 - 0.008 f'_c$;

ψ = Strength reduction factor for FRP = 0.85 ;

A_f = Cross sectional area of FRP strip; f_{fe} = stress level in FRP.

From Table 10, it can be seen that, ACI code procedure underestimates the actual ultimate moment strength of the slabs. The ratio of experimental to calculated ultimate moment of the 1.5m strengthened slabs ranged from (1.366 to 1.735) with average value of (1.553) and COV of (8.5%), whereas for 2m strengthened slabs ranged from (1.342 to 1.376) with average value of (1.358) and COV of (0.88%) was obtained. The lowest COV values mean less dispersion in the ratio of experimental to calculated ultimate moment, which also means a good representation of flexure strength prediction. The reason for which, the codes give less value than actual values is that, the assumed stress block of concrete used in the calculation of ultimate moment ACI code, include factor of safety.

Table (10): Measured and calculated ultimate moment strength.

OWS Slab Designation	$M_{u,exp.}$ kN.m	$M_{n,cal.}$ kN.m	$M_{u,exp.} / M_{n,cal.}$
1.5m OWS, d= 56mm, shear span=8.929			
S1	3.975	2.3	1.735
S1CF4	6.625	4.24	1.563
S1CF5	7.025	4.533	1.549
S1CF	7.65	5.6	1.366
2m OWS, d= 80mm, shear span=9.375			
S2	6.975	5.133	1.359
S2CF6	11.65	8.6	1.355
S2CF7	12.25	8.9	1.376
S2CF	13.15	9.8	1.342

* X= Mean, where:
X= **1.553** for 1.5m OWS and **1.358** for 2m OWS;
**SD= Standard deviation, where:
SD= **0.131** for 1.5m OWS and **0.012** for 2m OWS;
*** COV= Coefficient of Variant = (X / SD), where: COV= **8.5%** for 1.5m OWS and **0.88%** for 2m OWS.

However, the results showed by Table 10, indicate that the sand-PLWAC OWS exhibit a reduction in the load carrying capacity of a larger slab than of small slab. This is agreed with the results obtained by Wu et al. [5] for un-strengthened slabs. In contrast, the variation of the CFRP bond length in shear span (longer bond strength) shows a reverse effect on the strengthening ratio. This is because that the crack opening increased with increasing slab thickness, which lead to a considerable stress redistribution and energy release from the specimen [17]. In addition, according to Griffith, the probability of existing fictitious breaches is increased with increasing the specimen size, which leads to high stresses under the applied load causing a microscopic failure in their places[18]. In addition to that, the presence of LWA may lead to increase this probability.

3. Deflection

Deflection was measured at mid span of the slabs at different loading stages. The maximum deflections at failure were not obtained to avoid dial gauge damage. From figure 8, and after the linear range, it can be noticed that the strengthened 1.5m and 2m sand-PLWAC one way slabs exhibit less midspan deflection than control un-strengthened slab at all loading stages. This decrease in deflection for strengthened slabs is attributed to the bridging of the slab tension face provided by the bonded CFRP strips. Table 9 shows the measured and calculated service load deflection at midspan of the slabs. The service load is calculated by dividing the failure load by (1.6). It can be noticed that the calculated deflection is in general less than the measured one and the accuracy of the calculated deflection is decreased with increasing the length of the slab.

The mid-span deflection of the slabs at service load is calculated according to ACI 318-11 Code [4] method and the results are presented in Table 11. The effective second moment of area is to be found from equation:

$$I_e = \left(\frac{Mcr}{M}\right)^3 I_g + \left[1 - \left(\frac{Mcr}{M}\right)^3\right] I_{cr} \qquad \ldots\ldots. (3)$$

$$\Delta = K\left(\frac{M}{Ec * Ie}\right) L^2 \qquad \ldots\ldots. (4)$$

Where K is factor depend on type of loading and support condition.

The moment-deflection response for each slab is plotted in figure 9. It can be seen that the strength and stiffness of the strengthened slabs are increased with less ductility.. The reduction in ductility increased with increasing CFRP amount. The reduction in ductility can be attributed to the presence of CFRP which change the ductile behaviour of the control un-strengthened slabs to brittle (or less ductile) behaviour for the strengthened slabs.

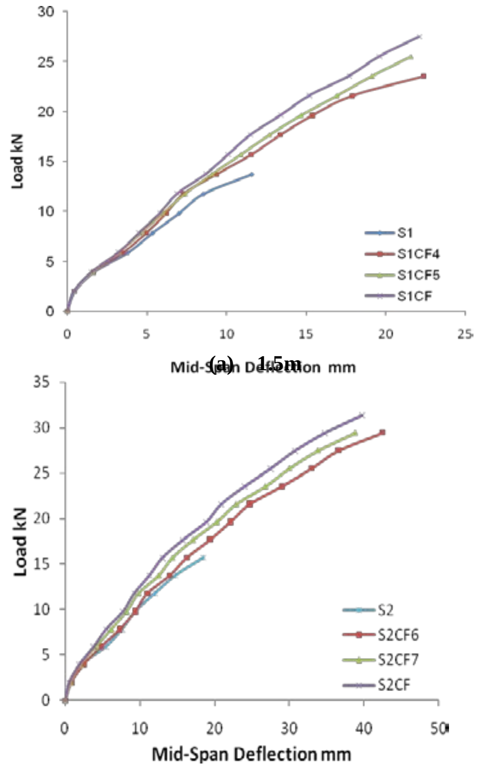

(b) 1.5m

Fig. (8): Load – midspan deflection curves.

Table (11): Measured and calculated midspan Deflections at service load of all sand-PLWAC OWS failed in flexure under static loading.

One Way Slab designation	Service Load (kN)	Measured Deflection (mm) (1)	Calculated Deflection (mm) (2)	Ratio (1)/(2)
S1	9.94	7.20	11.25	0.64
S1CF4	16.56	12.60	13.11	0.96
S1CF5	17.56	12.60	13.90	0.91
S1CF	19.13	13.20	11.02	1.19
S2	11.63	11.80	9.91	1.19
S2CF6	19.44	22.00	13.39	1.64
S2CF7	20.38	22.30	13.52	1.65
S2CF	21.94	21.00	13.34	1.57

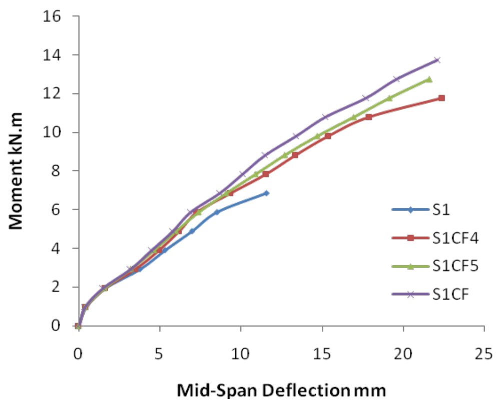

(a) 1.5m

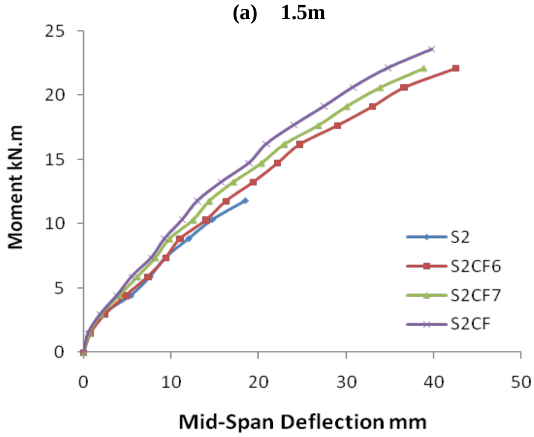

(b) 2m

Fig. (9): Moment – midspan deflection curves.

Also, figures 8 with Table 11 demonstrate that the deflection increases as the specimen size increases. Apart comparison between the moment- (midspan deflection-to-span ratio) (**Δ/L**) curves for the 1.5m and 2m OWS is presented in Fig. 10. The **Δ/L** was used as an indicator to span rotation. The midspan deflection-to-span ratio decreases with the increase in slab size. This implies that the ductility of slabs exhibit a reverse size effect, i.e., ductility decreases with the increase of size, namely, a large slab perform less ductility. This is agree with results obtained by Wu et al. [5] and Bazant [17].

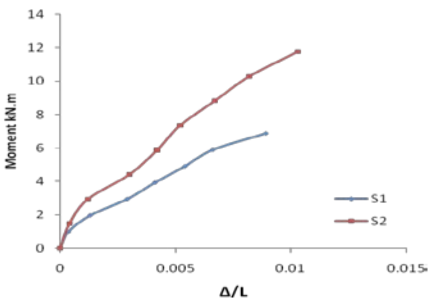

Fig. (10): Moment – midspan deflection –to- span ratio curves for sand PLWAC OWS.

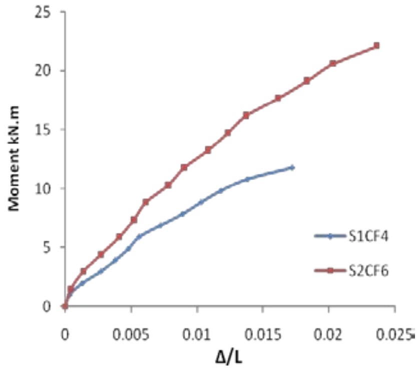

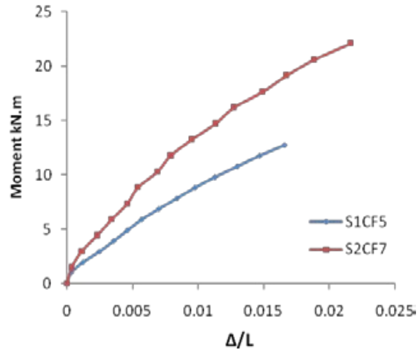

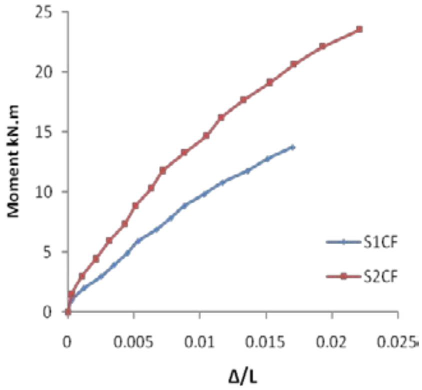

Fig. (10): Continued

Conclusions

The following conclusions can be drawn as follows**:**

1. In general higher ultimate loads were achieved for sand-PLWAC one way slabs strengthened with CFRP strips as compared with control un-strengthened slab under static loading. The strengthened sand-PLWAC OWS showed an increase in the ultimate load of about 78.0%, compared to the control un strengthened slabs.

2. The failure of sand-PLWAC OWS was by rupture of CFRP strips.
3. The sand-PLWAC one way slabs showed a reverse size effect on the flexural capacity of the slabs. The ultimate moment strength was decreased by (1.5% to 17.6%) with increase slab size. Therefore, this behaviour represented by the lower strengthening ratio and lower ductility with the increasing of slab size.

References

1. Duthinh, D., and Starnes, M., 2001, " Strength and Ductility of Concrete Beams Reinforced with Carbon FRP and Steel", National Institutes of Standard and Technology, Report no. 6830, USA, pp.59-72.
2. Zadeh, B., and Azmirad, H., 2005, " Structural Lightweight Concrete Production Using Eskandan Region Pumice", CI-Premier PTE LTD, 30th Conference on our World in Concrete & Structures: 23-24 August 2005, Singapore, Article no. ld:100030024, pp. 152-157.
3. NRMCA , 2006, "Concrete in Practice: What, Why and How?", CIP 36, Structural Lightweight Concrete, pp. 84.
4. ACI Committee-318, 2011, "Building Code Requirements for Structural Concrete (ACI 318M-11) and Commentary", American Concrete Institute, Farmington Hills, MI 48331, USA, pp. 30.
5. Wu, C.H., Kan, Y.C., Huang, C.H., Yen, T., and Chen, L.H., 2011, "Flexural Behavior and Size Effect of Full Scale Reinforced Lightweight Concrete Beam", Journal of Marine Science and Technology, Vol. 19, No. 2, pp. 132-140.
6. American Specifications for Testing Materials, ASTM C330-2004.
7. AL-Musawi, J.M., 2004, "Flexural Behavior of Porcelinite Reinforced concrete Beams", Ph.D. Thesis, University of Technology, Baghdad, Iraq.
8. SCGSM Laboratory Sheet, "Chemical Properties of Porcelinite Rock", the State Company of Geological Survey and Mining, Baghdad, Iraq.
9. ASTM A615/A615M-04b, "Standard Specification for Deformed and Plain carbon Steel Bars for Concrete Reinforcement", 2004, pp. 1-6.
10. Iraqi Standards No. 5/1984, "Ordinary Portland Cement", Ministry of Housing and Constructions, Baghdad, 2004.
11. Iraqi Standards No. 45/1984, "Aggregate from Natural Sources for Concrete and Construction", Ministry of Housing and Constructions, Baghdad, 2004.
12. Products Catalog, Innovation and Consistency, Product Data Sheet, Edition 6, 2010, Version No. 08. 06, pp. 65.
13. Manos, G.C., Stavroy, D.S., Dimosthenous, M.A., and kourtides, B., 2044, "Expermental and Analytical Investigation of Repaired and Strengthened Reinforced Concrete Structural Elements Utilizing CFRP", 13th World Conference on Earthquake Engineering , Vancouver, B. C., Canada, pp. 91.
14. Bonaldo, E., Barros, J.A., and Lourenco, P.B., 2007, "Influence of the Spacing Between NSM-CFRP Lamenates on the Flexural Strengthening Efficacy of RC Slabs", FRPRCS-8, University of Patras, Patras, Greece, pp. 1-11.
15. ACI Committee 440, 2002, "Guide for the Design and Construction of Externally Bonded FRP Systems for Strengthening Concrete Structures", ACI 440.2R-02, American Concrete Institute, pp. 31- 37.
16. Chiew, S.P., Sun, Q., and Yu, Y., 2007, "flexural Strength of RC Beams with GFRP Laminates", Journal of Composites for Construction, Vol. 11, No. 5, pp.361-372.
17. Bazant, Z.P., 1999, "Size effect on Structural Strength: A Review", Archive of Applied Mechanics 69, Office of Naval Research, N00014-91-J-1109, Northwestern University, Evanston, Illinois, USA, pp. 703-725.
18. مؤيد نوري الخلف, هناء عبد يوسف, " تكنولوجيا الخرسانة", قسم البناء والانشاءات, الجامعة التكنولوجية, بغداد, العراق, رقم الإيداع في المكتبة الوطنية ببغداد 997, 1982.